MOLECULAR AND CELLULAR BIOLOGY, Feb. 2011, p. 417–429 Vol. 31, No. 3
0270-7306/11/$12.00 doi:10.1128/MCB.00754-10

Early Recruitment of AU-Rich Element-Containing mRNAs Determines Their Cytosolic Fate during Iron Deficiency▽

Sandra V. Vergara,[1] Sergi Puig,[2] and Dennis J. Thiele[1]*

Department of Pharmacology and Cancer Biology, Duke University Medical Center, Research Drive-LSRC-C134, Durham, North Carolina 27710,[1] and Departamento de Biotecnología, Instituto de Agroquímica y Tecnología de Alimentos (CSIC), P.O. Box 73, E-46100 Burjassot, Valencia, Spain[2]

Received 29 June 2010/Returned for modification 19 July 2010/Accepted 22 November 2010

The yeast Cth2 protein is a $CX_8CX_5CX_3H$ tandem zinc finger protein that binds AU-rich element (ARE)-containing transcripts to enhance their decay in response to iron (Fe) deficiency. Mammalian members of this family of proteins are known to undergo nucleocytoplasmic shuttling, but little is known about the role of shuttling in the mechanism of ARE-dependent mRNA decay. Here we demonstrate that, like its mammalian homologues, Cth2 is a nucleocytoplasmic shuttling protein whose nuclear export depends on mRNA transport to the cytosol. The nuclear import information of Cth2 is contained within its tandem zinc finger domain, but it is independent of mRNA-binding function. Moreover, we also demonstrate that nucleocytoplasmic shuttling of Cth2 requires active transcription and that disruption of shuttling leads to defects in Cth2 function in mRNA decay under Fe deficiency. Taken together, our data suggest that under conditions of Fe deficiency Cth2 travels into the nucleus to recruit target mRNAs, perhaps cotranscriptionally, that are destined for cytosolic degradation as part of the mechanism of adaptation to growth under Fe limitation. These data also suggest an important role for nucleocytoplasmic shuttling in this conserved family of proteins in the mechanism of ARE-mediated mRNA decay.

Iron (Fe) participates in numerous biochemical processes, of which many are essential. Thus, under conditions of Fe scarcity, cells must ensure the appropriate allocation of Fe in order to meet essential metabolic needs while lowering its incorporation into proteins that participate in nonessential processes or proteins involved in metabolic pathways for which there are alternative salvage mechanisms (9, 16, 20, 23, 24, 26, 32). The *Saccharomyces cerevisiae* Cth1 and Cth2 proteins play a pivotal role in the cellular adaptation to Fe limitation by posttranscriptionally regulating Fe metabolism (23, 24).

Cth1 and Cth2 belong to the TTP (Tristetraprolin) family of mRNA-destabilizing proteins. Members of this family are characterized by an RNA-binding motif consisting of two tandem zinc fingers (TZFs) of the $CX_8CX_5CX_3H$ type, which directly interact with AU-rich elements (AREs) within the 3′ untranslated region of select groups of mRNAs (2, 3, 28, 29). This interaction leads to the rapid destabilization of the bound transcript in a process termed ARE-mediated mRNA decay (AMD). In response to Fe starvation, yeast Cth1 and Cth2 coordinately promote AMD of select groups of mRNAs, many of which encode proteins with functions in highly Fe-demanding processes such the tricarboxylic acid cycle, the mitochondrial electron transport chain, heme biogenesis, and Fe-S-containing proteins, presumably to allow prioritization of Fe utilization (23, 24, 32).

Studies have demonstrated that yeast AREs modulate poly(A) tail removal of a reporter mRNA, followed by decapping (31), and recent studies have demonstrated that Cth2-dependent AMD is catalyzed from the 5′ end to the 3′ end by the cytoplasmic exonuclease Xrn1 (20, 22). Similarly, studies have demonstrated that mammalian TTP promotes AMD by inducing poly(A) tail removal, followed by decapping and mRNA decay from both 5′→3′ and 3′→5′ directions (2, 4, 7, 12, 13, 15), suggesting a mechanistic conservation of AMD between yeast and mammals.

Despite progress in understanding the mechanisms of AMD, it remains largely unknown where TTP-related proteins recruit target transcripts or how they discriminate bona fide target transcripts from other ARE-bearing mRNAs. Subcellular localization experiments have revealed that mammalian TTP family members are nucleocytoplasmic shuttling proteins (17, 21), and although the importance of nucleocytoplasmic shuttling in the regulation of TTP-dependent AMD is not understood, it is interesting that stimulatory signals that activate TTP-dependent AMD (e.g., serum and lipopolysaccharide) also cause changes in the subcellular localization of TTP (3, 30). Therefore, nucleocytoplasmic shuttling of TTP may play a role in the mechanism of recognition of ARE-containing mRNAs destined for degradation.

Here we demonstrate that a yeast TTP family member, Cth2, is a nucleocytoplasmic shuttling protein whose nuclear export is mediated by mRNA export pathways. The nuclear import information of Cth2 is contained within the TZF domain, but it is independent of mRNA-binding function. We demonstrate that nucleocytoplasmic shuttling is important for Cth2-dependent AMD, as disruption of shuttling leads to defects in AMD and a growth defect under Fe-deficient conditions. Moreover, we present evidence suggesting that under Fe limitation, Cth2 travels into the nucleus to recruit ARE-containing transcripts destined for cytosolic degradation.

* Corresponding author. Mailing address: Department of Pharmacology and Cancer Biology, Duke University Medical Center, Research Drive-LSRC-C134, Durham, NC 27710. Phone: (919) 684-5776. Fax: (919) 668-6044. E-mail: dennis.thiele@duke.edu.

▽ Published ahead of print on 6 December 2010.

MATERIALS AND METHODS

Plasmids. For visualization of Cth2, the green fluorescent protein (GFP)-encoding sequence was inserted between the *CTH2* promoter and the *CTH2*

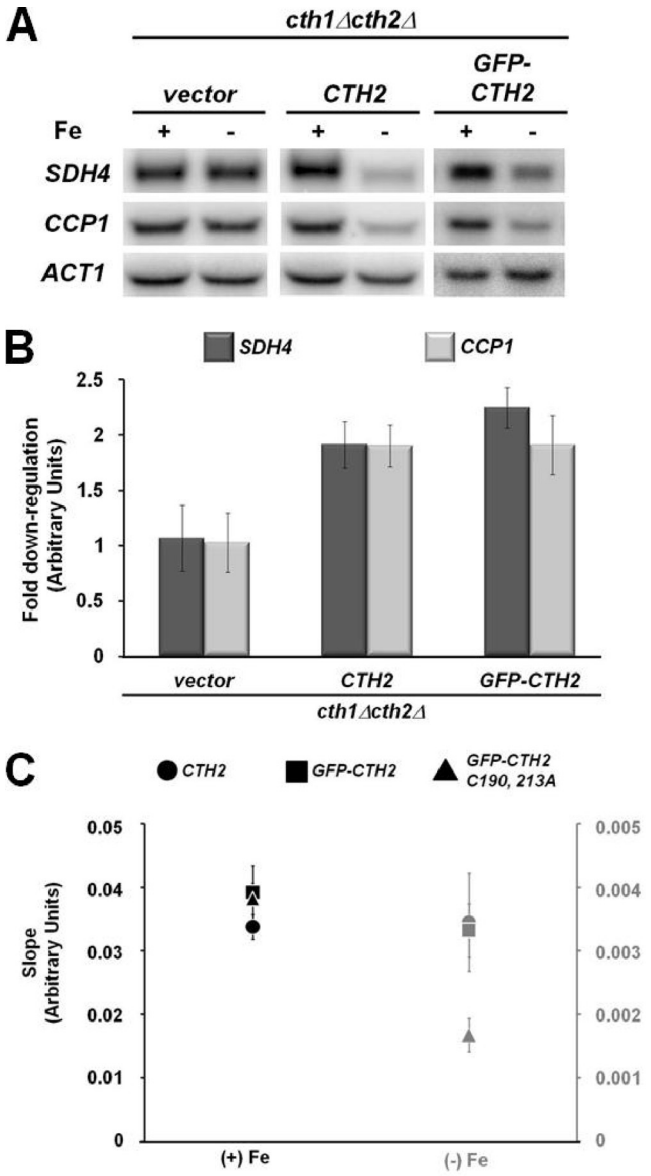

FIG. 1. Characterization of the GFP-Cth2 fusion protein. (A) *cth1*Δ *cth2*Δ mutant cells transformed with the vector pRS416-*CTH2* alone or with pRS416-*GFP-CTH2* were grown in medium containing 300 μM FAS (+Fe) or 100 μM BPS (−Fe), and total RNA was extracted and analyzed by RNA blotting as described by Puig et al. (23). (B) PhosphorImager quantification of steady-state levels of the *SDH4* and *CCP1* mRNAs from RNA blots from at least four independent experiments to determine the functionality of the epitope-tagged fusion. (C) *cth1*Δ *cth2*Δ mutant cells transformed with pRS416-*CTH2*, pRS416-*GFP-CTH2*, or the nonfunctional pRS416-*GFP-CTH2-C190,213A* fusion were reinoculated into medium containing iron (+Fe) or BPS (−Fe), and the slope of growth over 72 h under the specified conditions was analyzed.

coding sequence in a pRS416 plasmid backbone to produce a functional amino-terminal GFP-Cth2 fusion protein, assessed by the ability to promote the degradation of two well-characterized target mRNAs of Cth2 under Fe limitation (Fig. 1A). Fusing the epitope sequence at the carboxy terminus rendered Cth2 nonfunctional (data not shown). We used the "forced-localization" cassettes described by Edgington and Futcher (6), containing either two copies of the simian virus 40 (SV40) nuclear localization signal (NLS) or two copies of the protein kinase inhibitor (PKI) nuclear export signal (NES) to generate the NLS_2-*GFP-CTH2* and NES_2-*GFP-CTH2* fusions, respectively. Mutations within each cassette (see Fig. 6A and 7A) were introduced by site-directed mutagenesis to reverse the effect of the localization cassettes. The Flag-Cth2 fusion has been previously described (23). The *DCP2*-red fluorescent protein (RFP) fusion was a kind gift from Roy Parker at the University of Arizona, and the *YAP1*-GFP fusion was a kind gift from Anita Corbett at Emory University.

Live-cell microscopy. All microscopy experiments were done with live cultures and an AxioImager.A1 (Carl Zeiss, Thornwood, NY) with a 100×/1.4 Plan Apochromat oil immersion objective and an ORCA charge-coupled device camera (Hamamatsu, Bridgewater, NJ), and images were captured with the Metamorph 7.5 software. Overnight liquid cultures were reinoculated to an A_{600} of 0.2 in selective medium with a 100 μM concentration of the Fe chelator bathophenanthroline disulfonate (BPS) to induce Fe deficiency and robust expression of GFP-Cth2 fusion proteins. Temperature-sensitive strains were visualized at 24°C and after 1 h of incubation at 37°C. Thiolutin (Sigma T3450) was used at a concentration of 5 μg/ml for 30 min at 30°C. Cells were incubated for 30 min with 10 μg/ml 4′6-diamidino-2-phenylindole (DAPI) to stain yeast nuclei. Vacuoles (one or more per cell) may appear as clear indentations in differential interference contrast images and correspond to regions devoid of fluorescence signal. For cell quantification, at least 100 cells expressing fluorescence were analyzed for each experiment.

Yeast strains and growth assay. *xpo1-1*^{ts}, *mex67-5*^{ts}, *xpo1-1*^{ts}/*mex67-5*^{ts}, and *XPO1*/*MEX67* (isogenic wild type) strains were kindly provided by Karsten Weis at the University of California, Berkeley. *crm1-2* and *crm1-3* mutant strains were kindly provided by Anita Corbett at Emory University. The *xrn1*Δ (BY4741 *xrn1*::*KanMX4*) strain was obtained from Research Genetics. The *cth1*Δ *cth2*Δ mutant strain has been previously described (23). For growth assay (see Fig. 8B), overnight cultures of *cth1*Δ *cth2*Δ mutant cells expressing pRS416-GFP-CTH2 (WT) and GFP-CTH2-C190,213A, as well as fusions with the appended NLS_2 and NES_2 cassettes, and their inactivated forms were reinoculated to an A_{600} of 0.05 in synthetic complete medium lacking uracil and leucine (SC-Ura-Leu) in the presence of either 300 μM ferrous ammonium sulfate (FAS; +Fe) or 100 μM BPS (−Fe). A_{600} was measured every 12 h for 72 h, and growth was analyzed by comparing the slopes. Experiments were done in triplicate.

Nuclear fractionation and RNA analyses. Nuclei were separated from the cytosolic fraction by differential centrifugation. Overnight cultures of *cth1*Δ *cth2*Δ mutant cells cotransformed with plasmids pRS416-FLAG-CTH2 and pRS415 were reinoculated to an A_{600} of 0.2 into 200 ml of SC-Ura-Leu, split into two 100-ml subcultures to which either 300 μM FAS (+Fe) or 100 μM BPS (−Fe) was added, and grown at 30°C for 6 h. Spheroplasting and cell lysis were carried out with reagents from the MITOISO3 kit from Sigma. Differential centrifugation was carried out at 3,500 × *g* for 10 min to obtain unlysed whole cells and at 20,000 × *g* for 20 min to isolate nuclei, the cytosolic fraction was collected, and the fractions were analyzed by immunoblotting with antibodies against the FLAG epitope (Sigma F-8592), the nucleus-resident protein Nop1 (Covance MMS-581), and the cytosolic protein Pgk1 (Molecular Probes A6457). RNA analyses were performed as previously described by Puig et al. (23).

RESULTS

Cth2 is a nucleocytoplasmic shuttling protein. TTP promotes AMD by interacting with members of the cytosolic general mRNA decay machinery (4, 12, 13, 15). While TTP stimulates cytosolic mRNA degradation, experiments reveal that TTP shuttles between the nucleus and cytosol (17, 21). Similarly, in *S. cerevisiae*, Cth2 can promote AMD by recruiting the cytosolic 5′→3′ decay machinery (20). To establish the subcellular localization of Cth2, a combination of live microscopy and biochemical fractionation experiments was carried out with cells expressing functional GFP or FLAG epitope-tagged proteins. The functionality of the GFP fusion protein was assessed by testing its ability to promote the degradation of two well-characterized target mRNAs of Cth2 under Fe limitation (Fig. 1A). Quantification of the *n*-fold downregulation of the *SDH4* and *CCP1* mRNAs under Fe deficiency from at least three independent experiments is shown in Fig. 1B. In addition, we cultured *cth1*Δ *cth2*Δ mutant cells expressing Cth2, GFP-Cth2, or the non-mRNA-binding mutant protein GFP-

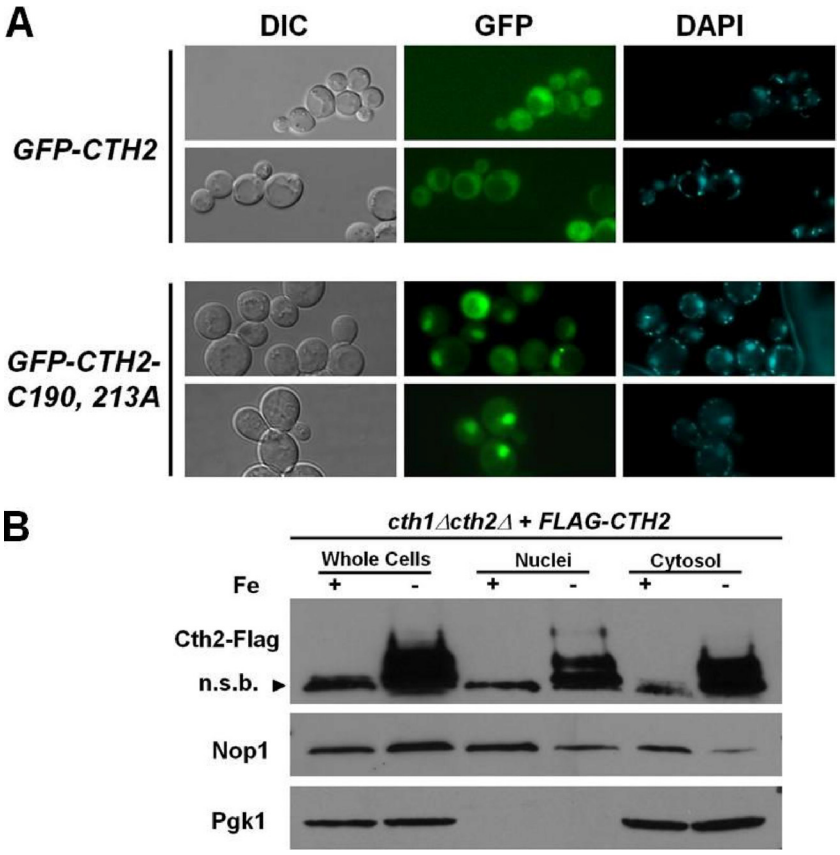

FIG. 2. Cth2 is a cytosol- and nucleus-resident protein. (A) GFP-Cth2 is expressed diffusely throughout cells, while a non-mRNA-binding mutant protein is largely localized to the nucleus. *cth1*Δ *cth2*Δ mutant cells transformed with pRS416-*GFP-CTH2* (top) or pRS416-*GFP-CTH2-C190,213A* (bottom) were visualized by live fluorescence microscopy. DAPI was used to stain nuclei. (B) Cth2 is a nucleus- and cytosol-resident protein. Nuclear and cytosolic fractions were obtained from *cth1*Δ *cth2*Δ mutant cells expressing pRS416-*FLAG-CTH2* grown as in Fig. 1A and analyzed by immunoblotting. The anti-FLAG horseradish peroxidase-conjugated antibody used to detect Flag-Cth2 also detects a nonspecific band (n.s.b.) indicated by the arrowhead. Nuclear and cytosolic fractions were identified by incubation with antibodies against the Nop1 and Pgk1 proteins, respectively. DIC, differential interference contrast.

Cth2-C190,213A (23) and compared their growth under Fe-deficient conditions. As shown in Fig. 1C, cells expressing the non-mRNA-binding mutant protein GFP-Cth2-C190,213A are compromised for growth under Fe-deficient conditions compared to cells expressing the untagged *CTH2* or the *GFP-CTH2* fusion (minus Fe; gray graph). More importantly, growth under Fe deficiency is almost indistinguishable between *CTH2*- and *GFP-CTH2*-expressing cells, suggesting that the GFP epitope-tagged version of Cth2 is functional. All cells grew equally well in the presence of Fe (plus Fe; black graph). The functionality of the Flag-Cth2 protein has been previously demonstrated (23).

Cells transformed with a *GFP-CTH2* fusion were grown under Fe limitation conditions to induce expression of the protein. Live fluorescence microscopy showed that GFP-Cth2 is localized diffusely throughout cells (Fig. 2A, top). We previously demonstrated that mutations in two cysteine residues within the TZF domain of Cth2 (Cys190 and Cys213) eliminate the interaction between Cth2 and ARE sequences within target mRNAs, which in turn abolishes the ability of Cth2 to promote AMD (23). To determine whether the ability to interact with mRNA impacts Cth2 localization, we localized the GFP-Cth2-C190,213A fusion protein by live fluorescence microscopy. As shown in Fig. 2A (bottom), the GFP-Cth2-C190,213A mutant protein is largely localized to the nuclei of over 84% of the cells observed, in comparison to the GFP-Cth2 fusion. To independently assess the localization of Cth2, cells expressing a Flag-Cth2 fusion protein were grown under Fe-replete or Fe-deficient conditions and nuclei were separated from cytosol by differential centrifugation (Fig. 2B). As previously demonstrated, Flag-Cth2 is readily detected only in extracts from cells treated under Fe deficiency conditions (23) (Fig. 2B). Immunoblotting analysis of fractions enriched for nuclei show that Flag-Cth2 cofractionates with the nucleus-resident protein Nop1. In addition, both Flag-Cth2 and the cytosolic protein Pgk1 can be detected in the cytosolic fraction (Fig. 2B). These results demonstrate that Cth2 is both a cytosol- and a nucleus-resident protein.

Localization experiments for TTP and related proteins demonstrated that these proteins actively shuttle between the nucleus and the cytosol and that their export from the nucleus relies on the export receptor Crm1/Xpo1 (17, 21). We tested whether translocation of Cth2 out of the nucleus was Crm1/Xpo1 dependent by visualizing the GFP-Cth2 fusion in a yeast

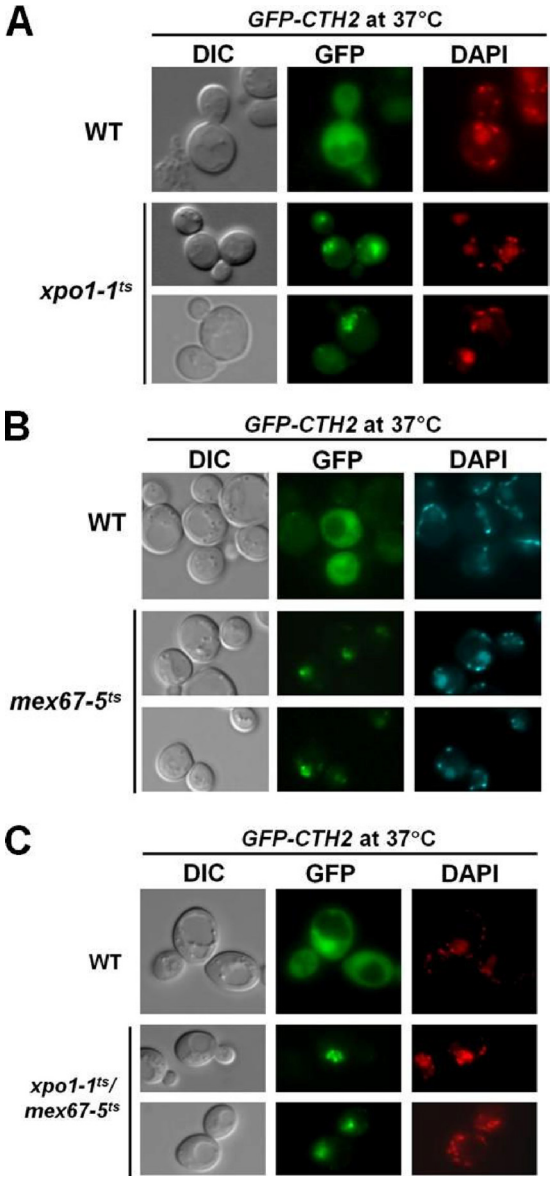

FIG. 3. Cth2 is a nucleocytoplasmic shuttling protein. Wild type (WT) and thermosensitive *xpo1-1*^{ts} (A), *mex67-5*^{ts} (B), and *xpo1-1*^{ts} *mex67-5*^{ts} double mutant strains (C) transformed with pRS416-*GFP-CTH2* were grown at 24°C and visualized after a 1-h shift to 37°C to disrupt the function of the Xpo1-1 and Mex67-5 mutant proteins. DIC, differential interference contrast.

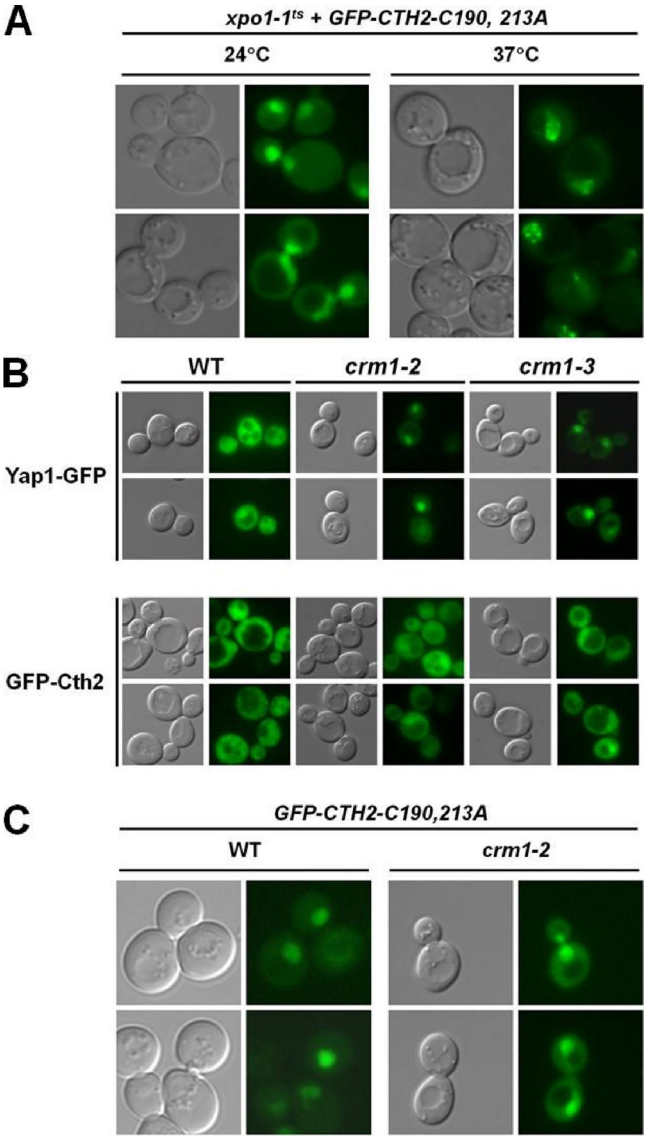

FIG. 4. Cth2 is not a direct cargo protein of Xpo1/Crm1. (A) Thermosensitive strain *xpo1-1*^{ts} transformed with pRS416-*GFP-CTH2-C190,213A* was visualized at 24°C and after a 1 h shift to 37°C to disrupt the function of Xpo1-1. (B) Wild type, *crm1-2* and *crm1-3* mutant strains were transformed with plasmids *YAP1-GFP* and p416-*GFP-CTH2*, and grown under Fe deficiency for 6 h at 30°C prior to visualization. (C) Wild type and *crm1-2* strains were transformed with pRS416-*GFP-CTH2-C190,213A* and visualized under the same conditions as in panel B.

strain harboring a temperature-sensitive allele of the essential nuclear export receptor Crm1/Xpo1 (*xpo1-1*^{ts}). As shown in Fig. 3A, the GFP-Cth2 fusion protein partially accumulates in the nuclei of *xpo1-1*^{ts} mutant cells incubated at the restrictive temperature (37°C) but not in those of wild-type cells, consistent with the notion that Cth2 export from the nucleus is at least partially dependent on Crm1/Xpo1. Disruption of the Cth2-mRNA interaction leads to a partial nuclear accumulation of the GFP-Cth2 fusion (Fig. 2A, bottom). Thus, we asked whether full-length Cth2 localization was also defective in a strain harboring a temperature-sensitive allele of the general mRNA export factor Mex67. As shown in Fig. 3B, GFP-Cth2 is retained in the nuclei of cells of the *mex67-5*^{ts} mutant strain at 37°C but not in those of wild-type cells grown under the same conditions, and this nuclear retention defect is exacerbated in a strain harboring both *xpo1-1*^{ts} and *mex67-5*^{ts} mutations grown at the restrictive temperature but not in wild-type cells (Fig. 3C). In addition, the nuclear accumulation of the GFP-Cth2-C190,213A mutant protein increases in combination with the *xpo1-1*^{ts} mutation at 37°C (Fig. 4A), which might be consistent with a mechanism whereby Cth2 is exported from the nucleus via two pathways: one that is mRNA export dependent and a second pathway that is NES dependent.

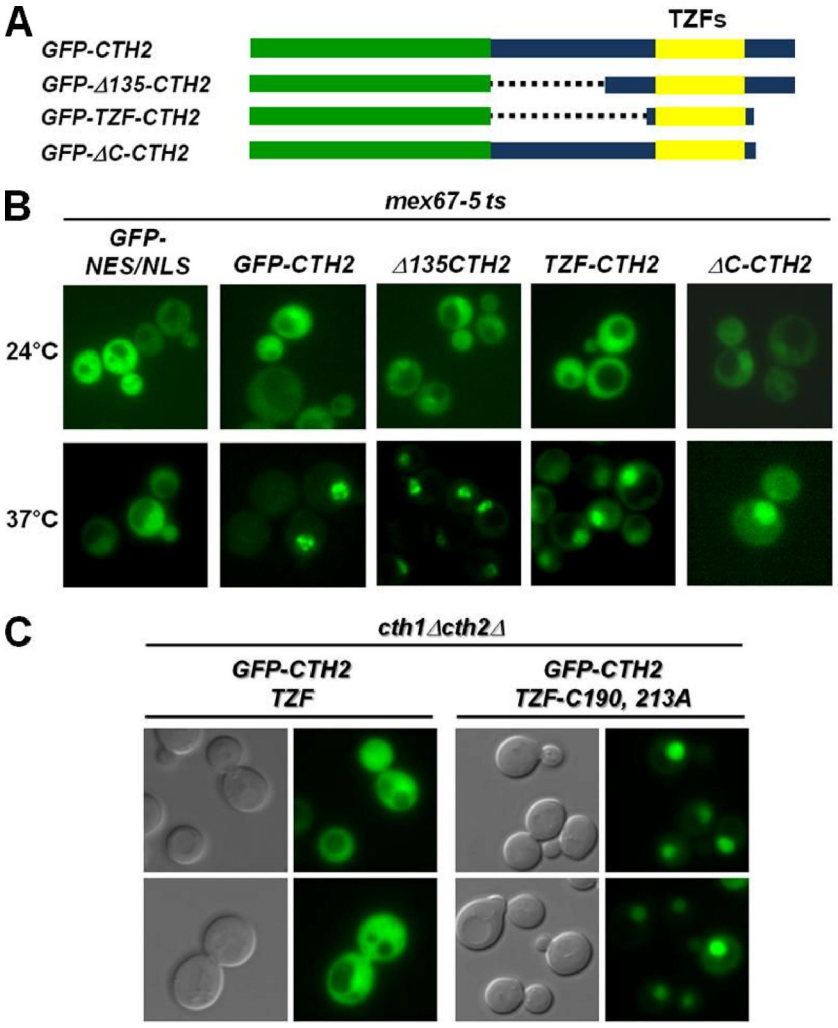

FIG. 5. The nuclear import information of Cth2 is localized within its mRNA binding domain. (A) Representation of the *GFP-CTH2* fusion and truncations made at the amino and carboxy termini. GFP is indicated in green, Cth2 in blue, and tandem zinc finger domain (TZFs) is indicated in yellow. (B) *mex67-5*^{ts} cells were transformed with plasmid *GFP-NES/NLS* as a control and plasmids containing full-length *GFP-CTH2* and the truncations described above. All cells were visualized at 24°C and after a 1 h shift to 37°C. (C) *cth1*Δ *cth2*Δ mutant cells transformed with *GFP-TZF-CTH2* and the non-mRNA-binding mutant *GFP-TZF-CTH2-C190,213A*.

Although the regions of TTP containing the NES and NLS sequences are not conserved in yeast Cth2, sequence alignments identified conserved regions among fungi that might act as localization sequences. A series of truncations of the Cth2 amino terminus, carboxy terminus, or both were generated based on the conserved regions (Fig. 5A) and localized in the context of a GFP fusion in order to identify a possible NES. However, none of the truncations exhibited an apparent defect in localization in wild-type cells (data not shown). *In situ* hybridization experiments have demonstrated that poly(A) RNA export is defective in *xpo1-1*^{ts} mutant cells incubated at 37°C for 15 min (27), raising the possibility that the nuclear export defect of GFP-Cth2 in the *xpo1-1*^{ts} mutant strain might be independent of the NES-mediated transport deficiency and instead be a consequence of the poly(A) RNA retention phenotype of this strain. Additional alleles of *CRM1*/*XPO1* that do not display a defect in poly(A) RNA export but are defective in NES-mediated transport have been isolated (18). Unlike the *xpo1-1*^{ts} mutant strain, the *crm1-2* and *crm1-3* mutant strains are not temperature sensitive and present no overt growth defects, even at 37°C (19). Therefore, we used the *crm1-2* and *crm1-3* mutant strains to ascertain whether GFP-Cth2 localization is defective when only the NES-dependent nuclear export pathway is disrupted. Interestingly, GFP-Cth2 localization is not affected in the *crm1-2* or *crm1-3* mutant strain (Fig. 4B), even after incubation at 37°C (data not shown), while, as expected, shuttling of the well-characterized NES-containing protein Yap1-GFP is disrupted in the same strains. Moreover, localization of the non-mRNA-binding mutant protein GFP-Cth2-C190,213A does not change in the *crm1-2* strain (Fig. 4C). Together, these data suggest that GFP-Cth2 export from the nucleus is solely dependent on RNA export pathways and independent of NES-mediated transport.

The nuclear import information of Cth2 is located within the mRNA-binding domain. Visualization of the truncated protein fusions described in Fig. 5A in the *mex67-5*^{ts} mutant

strain allowed the determination of the nuclear import information within Cth2. As shown in Fig. 5B, none of the truncations showed an obvious difference in localization compared to GFP-Cth2 in cells grown at 24°C (top panels), but inactivation of the mRNA export activity of the *mex67-5*^{ts} mutant by incubation at 37°C for 1 h clearly showed nuclear accumulation of GFP-Cth2 and the three truncation variants (Fig. 5B, bottom panels). A GFP epitope fused to an NLS and an NES sequence was used as a control and showed no nuclear accumulation under the same conditions. These data suggest that the minimal nuclear import information in Cth2 resides within the TZF motif region. Moreover, mutations known to disrupt the TZF-mRNA interaction cause the nearly complete nuclear accumulation of the TZF fusion protein in the *cth1*Δ *cth2*Δ mutant strain (Fig. 5C).

Taken together, these results demonstrate that Cth2 is a nucleocytoplasmic shuttling protein and that Cth2 export from the nucleus is dependent on nuclear mRNA export pathways. In addition, our data indicate that the mRNA binding domain contains the minimal nuclear import information of Cth2 as in mammalian TTP (17, 21).

Nucleocytoplasmic shuttling of Cth2 is important for function in AMD. While we identified the TZF as the region containing the minimal nuclear import information, mutations within this domain abolish the mRNA-binding activity of Cth2 (data not shown), precluding the determination of whether nuclear localization alone, rather than an additional contribution from mRNA binding, plays a role in Cth2 function. In order to ascertain the importance of Cth2 nucleocytoplasmic shuttling in AMD, we altered the steady-state localization of Cth2 by attaching forced-localization cassettes (6) consisting of two copies of the SV40 NLS sequence or two copies of the PKI NES sequence at the amino terminus of the GFP-Cth2 fusion. As controls, localization cassettes in which we introduced mutations within key functional residues were fused to GFP-Cth2, thus rendering the localization sequences inactive (Fig. 6A and 7A). To assay the effectiveness of the appended sequences, we visualized the localization of the NLS_2-GFP-Cth2 fusion and its inactive form in a wild-type strain by live fluorescence microscopy. As shown in Fig. 6B, the NLS_2-GFP-Cth2 protein is predominantly localized to the nuclei of over 73% of the cells observed (Fig. 6C), while the GFP-Cth2 and inac-NLS_2-GFP-Cth2 proteins are localized throughout the cells, displaying nuclear accumulation in a mere 4% and 17% of the cells observed, respectively (Fig. 6C).

Due to the difficulty of visualizing nuclei devoid of detectable fluorescence by live microscopy in wild-type yeast, we evaluated the efficacy of the NES_2-GFP-Cth2 fusion in the *mex67-5*^{ts} mutant strain after a 1-h shift to the nonpermissive temperature in order to disrupt mRNA export. As shown in Fig. 7B, cytosolic localization of the NES_2-GFP-Cth2 fusion is greater than that of the GFP-Cth2 or inac-NES_2-GFP-Cth2 fusion in the *mex67-5*^{ts} mutant strain at 37°C. While the NES_2-GFP-Cth2 fusion appeared localized to the nuclei of only 11% of the cells visualized, GFP-Cth2 accumulated in the nuclei of approximately 96% of the cells observed and the inac-NES_2-GFP-Cth2 fusion protein accumulated in the nuclei of approximately 63% of the cells analyzed. These data demonstrate that both of the appended localization sequences disrupt the native localization of GFP-Cth2 and that fusions harboring inactivating mutations within the forced-localization cassettes more closely resemble the localization of wild-type GFP-Cth2.

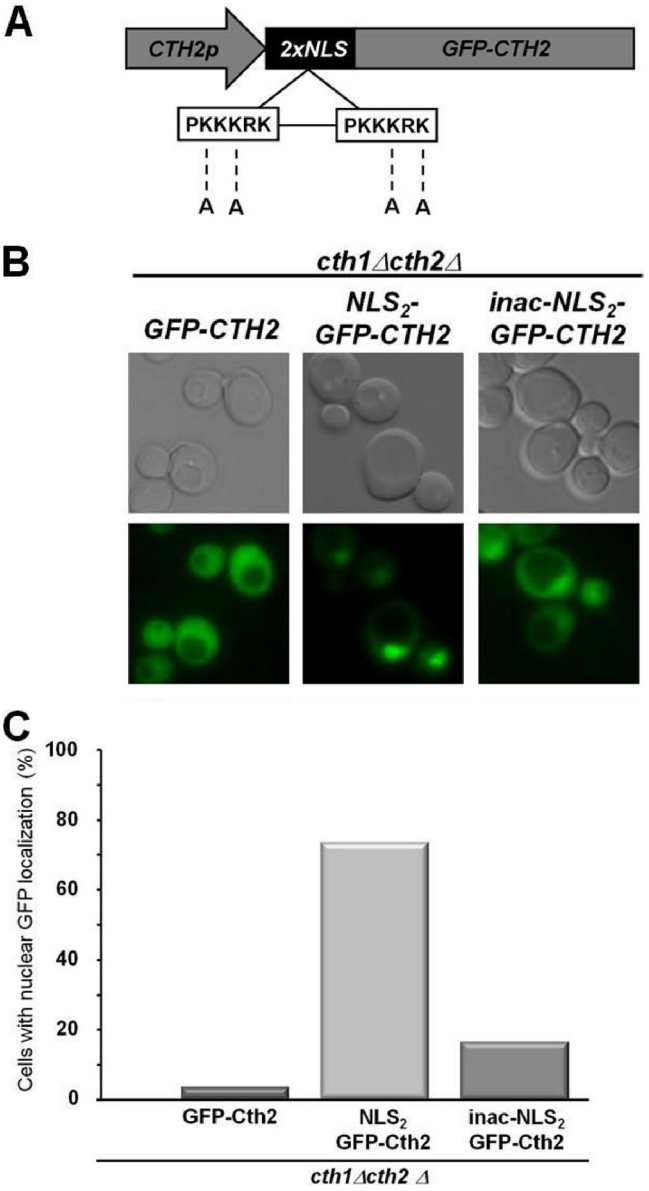

FIG. 6. Fusion of a tandem NLS cassette efficiently shifts the equilibrium of Cth2 expression to the nucleus. (A) Representation of the forced nuclear localization fusion. Two tandem copies of the SV40 NLS sequence were inserted between the *CTH2* promoter and the *GFP-CTH2* fusion. The active SV40 NLS sequence is shown the box, and the specific lysines mutated to alanines to inactivate the NLS sequence are shown. (B) *cth1*Δ *cth2*Δ mutant cells transformed with p416-*CTH2p-GFP-CTH2*, p416-*CTH2p-NLS*$_2$*-GFP-CTH2*, or p416-*CTH2p-inacNLS*$_2$*-GFP-CTH2* were grown under Fe-deficient conditions and visualized by live fluorescence microscopy. (C) Percentage of cells in which the indicated fusion protein is localized to the nucleus. At least 100 cells were observed per experiment.

To assess how localization might influence Cth2 function, we analyzed the steady-state levels of the *SDH4* transcript in cells competent for mRNA export and degradation (as in Fig. 1A) but expressing the fusion proteins described in Fig. 6A and 7A (Fig. 8A). In addition, we asked whether altering the native

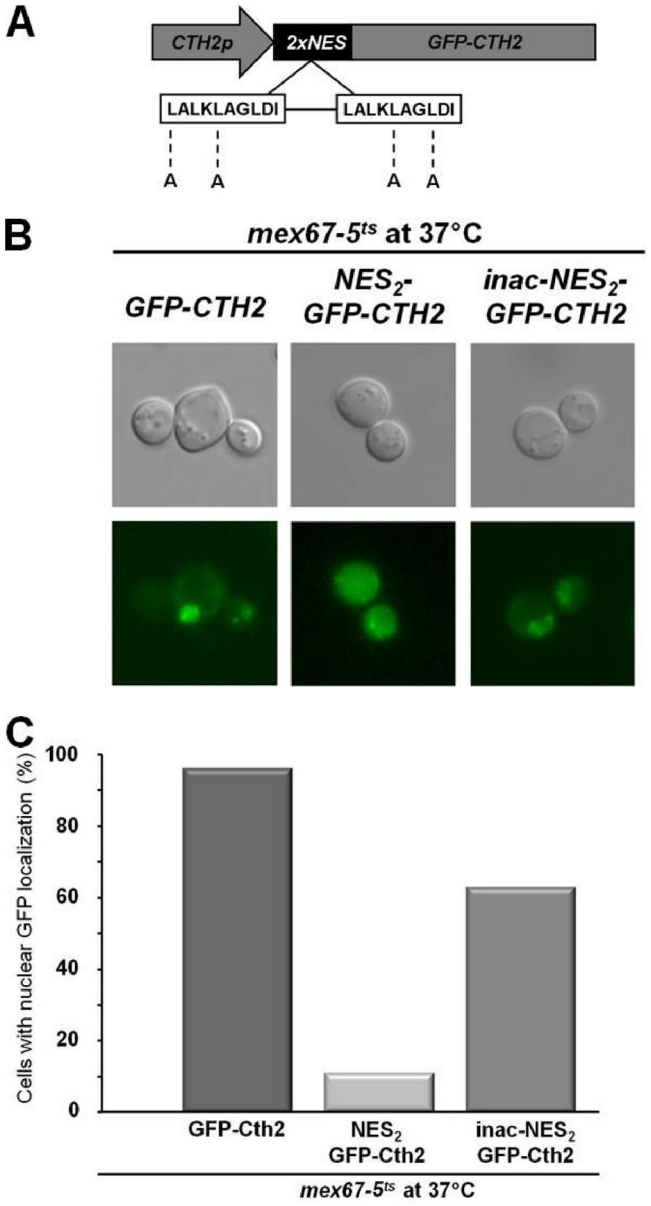

FIG. 7. Fusion of a tandem NES cassette efficiently shifts the equilibrium of Cth2 expression to the cytosol. (A) Representation of the forced nuclear export fusion. Two tandem copies of the PKI NES sequence were inserted between the *CTH2* promoter and the *GFP-CTH2* fusion. The active PKI NES sequence is shown the box and the specific leucines mutated to alanines to inactivate the NES sequence are shown. (B) *mex67-5*^{ts} cells transformed with p416-*CTH2p-GFP-CTH2*, p416-*CTH2p-NES*$_2$*-GFP-CTH2*, or p416-*CTH2p*-inac*NES*$_2$*-GFP-CTH2* were grown under Fe-deficient conditions at 24°C and visualized after a 1-h shift to 37°C by live fluorescence microscopy. (C) Percentage of cells in which the indicated fusion protein is localized to the nucleus. At least 100 cells were observed per experiment.

localization of Cth2 affects cell growth under Fe deficiency conditions (Fig. 8B). Cells expressing the GFP-Cth2 protein show a decrease in *SDH4* mRNA levels, while cells expressing the nonfunctional mutant protein GFP-Cth2-C190,213A or the appended NLS_2 and NES_2 cassettes harbor defects in the downregulation of the *SDH4* mRNA (~1-, 1.5-, and 1.7-fold changes, respectively). Inactivation of the localization sequences (inac-NLS_2 and inac-NES_2) rescues the downregulation defect to near wild-type levels (roughly 2.3- and 2.7-fold changes, respectively, Fig. 8A). Consistent with these data, cells expressing the NLS_2-GFP-Cth2 and NES_2-GFP-Cth2 proteins are compromised for growth under Fe-deficient conditions compared to cells expressing the GFP-Cth2 protein or the inactivated NLS_2 and NES_2 forms (triangles, Fig. 8B). Cells expressing any of these fusion proteins grow equally well in the presence of abundant Fe (diamonds, Fig. 8B), conditions under which Cth2 activity is not required and it is therefore not expressed (23). Immunoblotting experiments demonstrate that the expression levels of all GFP fusion proteins are relatively equivalent (Fig. 8C). Cth2, like all of its mammalian counterparts, is phosphorylated (our unpublished results), and investigations of the role of phosphorylation are under way. Interestingly, we found that forced relocalization of GFP-Cth2 resulted in changes in the phosphorylation state of the fusion proteins. As shown in Fig. 8C, the NLS_2-GFP-Cth2 fusion is hypophosphorylated while the NES_2-GFP-Cth2 protein is hyperphosphorylated. Inactivation of the localization cassettes caused the reversal of the phosphorylation state of these fusion proteins, which more closely resembled the phosphorylation of GFP-Cth2. Lastly, the GFP-Cth2-C190,213A mutant protein, which is partially nuclear, appears to have a partial defect in phosphorylation (Fig. 8C). The ability of the inactivated localization sequences to rescue both the Fe deficiency growth phenotype and the downregulation defect of the *SDH4* mRNA indicates that the appended sequences do not interfere with Cth2 function in mRNA binding or degradation. Moreover, our data suggest that Cth2 is posttranslationally modified differently in the nuclear and cytosolic compartments.

Recent studies have demonstrated that Cth2 promotes Fe deficiency-dependent degradation of the *SDH4* mRNA in the 5′→3′ direction, which is catalyzed by the cytosolic exonuclease Xrn1 (20). Deletion of the *XRN1* gene causes the accumulation of cytoplasmic P bodies, as mRNAs fail to be degraded and accumulate within these structures. While GFP-Cth2 localizes throughout wild-type cells, it accumulates in P bodies in strains deleted for the *XRN1* gene (20). This suggests that the function of Cth2 in promoting AMD may be the delivery of the target transcripts to the cytosolic 5′→3′ degradation machinery and that degradation of the target mRNA is required for release of Cth2, perhaps to engage in another round of mRNA delivery. To ascertain whether disruption of nucleocytoplasmic shuttling affects Cth2 localization to P bodies, we visualized the NLS_2-GFP-Cth2 and NES_2-GFP-Cth2 proteins (as well as their inactivated forms) in the *xrn1*Δ mutant strain. As previously demonstrated (20) and shown in Fig. 9A, GFP-Cth2 colocalizes with the P-body-resident protein Dcp2-RFP in the *xrn1*Δ mutant strain in approximately 88% of the cells observed. Our experiments revealed that forced mislocalization of Cth2 greatly impaired its ability to localize to P bodies. As shown in Fig. 9A, the NLS_2-GFP-Cth2 fusion localizes to P bodies in approximately 3.5% of the cells observed, while its inactivated form shows P-body localization in 77% of the cells analyzed. Similarly, the NES_2-GFP-Cth2 fusion protein showed P-body localization in only 26% of the cells visualized, while inactivation of the NES cassette allowed its localization to P bodies in approximately 73% of the cells observed.

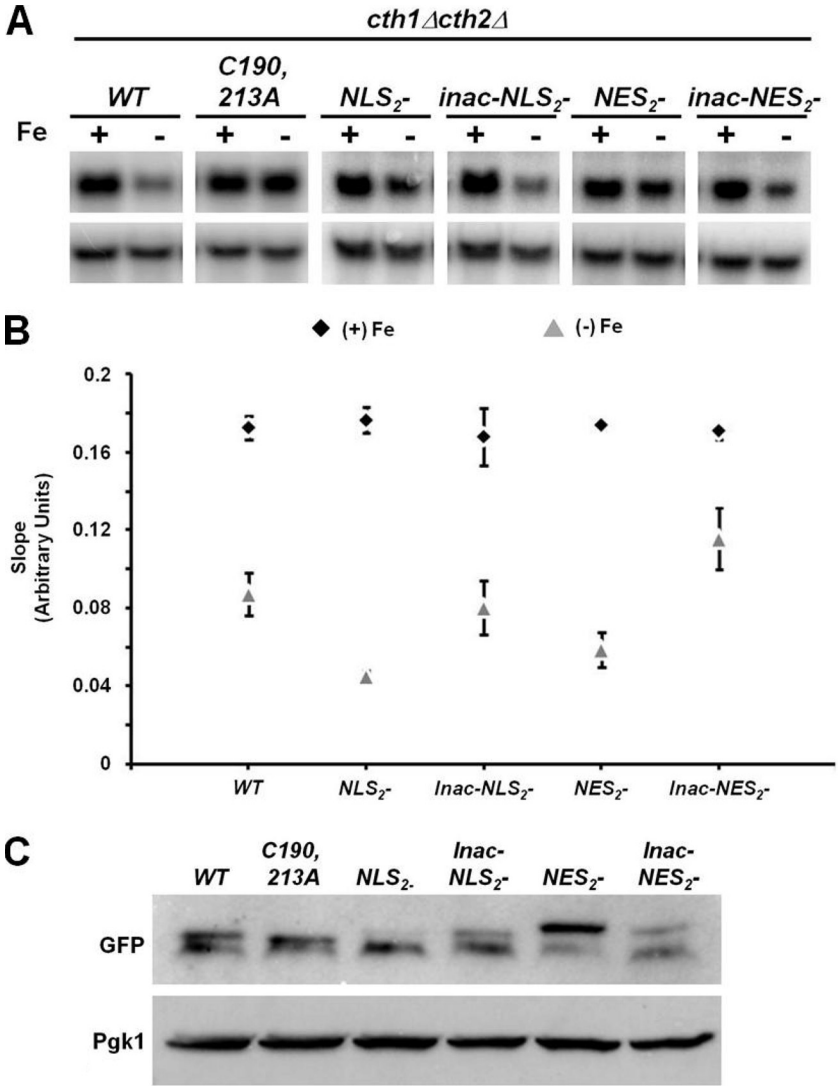

FIG. 8. Alterations in steady-state localization compromises Cth2 function. (A) *cth1*Δ *cth2*Δ mutant cells were transformed with *GFP-CTH2* (WT), *GFP-CTH2-C190,213A* mutant (C190,213A), or the forced-localization fusions described in Fig. 6A and 7B (NLS_2, $inacNLS_2$, NES_2, and $inacNES_2$). Transformants were grown in +Fe or −Fe conditions and steady-state levels of the *SDH4* transcript were analyzed by RNA blotting. (B) Cells transformed with the indicated fusion proteins were grown under +Fe or −Fe conditions for 72 h. A_{600} was measured every 12 h and growth was analyzed by comparing the slopes. Experiment was done in triplicate; error bars represent standard deviation. (C) Cells transformed with the indicated fusions were grown under −Fe conditions for 6 h, total protein extracted and analyzed by immunoblotting.

In addition to disrupting mRNA binding, mutation of cysteine residues within the TZF domain region of TTP and Cth2 causes their nuclear accumulation (17) (Fig. 2A), suggesting that the interaction of TTP and Cth2 with their cognate target mRNAs is important for nuclear export. Interestingly, visualization of the GFP-Cth2-C190,213A mutant protein in *xrn1*Δ mutant cells demonstrates that localization to P bodies also depends on the Cth2-mRNA interaction. As shown in Fig. 9B, while GPF-Cth2 colocalizes with the P-body component protein Dcp2-RFP in *xrn1*Δ mutant cells, the mRNA binding-incompetent mutant protein GFP-Cth2-C190,213A is largely retained in the nucleus, similar to its localization in wild-type cells (Fig. 2A, bottom). Moreover, fusion of the NES cassette at the amino terminus of the GFP-Cth2-C190,213A protein failed to restore the localization to P bodies (Fig. 9C), and inactivation of the NES sequences (as described in Fig. 7A) reversed its localization back to the nucleus. These data suggest that mRNA binding and shuttling out of the nucleus precede Cth2 localization to cytosolic P bodies in the *xrn1*Δ mutant strain. Together, these results demonstrate that, like its mammalian homologs, Cth2 actively moves between the nucleus and the cytosol. Furthermore, these results suggest that the ability of Cth2 to move between both compartments is important for function, indicating that nucleocytoplasmic shuttling may be an integral component of the AMD-promoting activity of Cth2.

Cytosolic localization of Cth2 depends on mRNA synthesis. If Cth2 binds target mRNAs in the nucleus, disruption of RNA synthesis by inhibiting transcription could prevent Cth2 nucleocytoplasmic shuttling and, consequently, might also prevent the accumulation of Cth2 in P bodies. To investigate GFP-

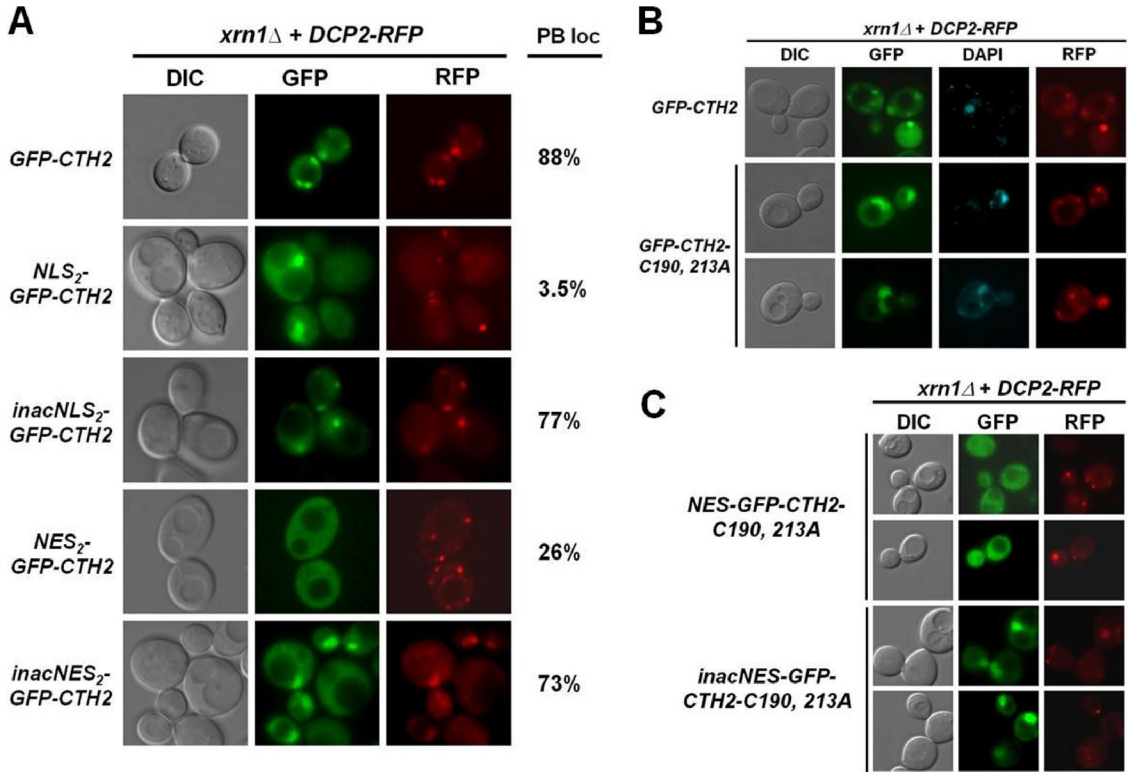

FIG. 9. Alterations in steady-state localization compromises Cth2 function. (A) Disruption of native localization of Cth2 prevents its accumulation in P bodies. *xrn1*Δ mutant cells were cotransformed with pRS416-*DCP2-RFP* and p416-*CTH2p-GFP-CTH2* (WT) or the forced-localization fusions described in Fig. 6A and 7A. The percentage of cells in which the specified fusion showed P-body localization (PB loc) is indicated. (B) P-body localization of Cth2 requires interaction with mRNA. *xrn1*Δ mutant cells were cotransformed with pRS416-*DCP2-RFP* and pRS416-*GFP-CTH2* or non-mRNA-binding plasmid pRS416-*GFP-CTH2-C190,213A*. (C) Forced localization of the non-mRNA-binding mutant protein to the cytosol does not rescue its localization to P bodies. The NES_2 cassette or its inactivated form described in Fig. 7A were attached at the amino terminus of the *GFP-CTH2-C190,213A* fusion and their localization analyzed in *xrn1*Δ mutant cells. All cells were visualized after 6 h of growth under Fe-deficient conditions.

Cth2 localization in the absence of ongoing mRNA synthesis, we used a yeast strain expressing a temperature-sensitive allele of the large subunit of RNA polymerase II (*rpb1-1*^{ts}) and, independently, a pharmacological inhibitor of transcription (thiolutin). As shown in Fig. 10A, GFP-Cth2 accumulates in the nuclei of *rpb1-1*^{ts} mutant cells incubated at 37°C, while it remains localized throughout cells grown at the permissive temperature. Moreover, incubation of wild-type cells with the transcription inhibitor thiolutin also resulted in nuclear retention of GFP-Cth2. GFP fused to an NLS/NES sequence does not show nuclear accumulation under the same conditions (Fig. 10B). Poly(A) binding protein 1 (Pab1) is a nucleocytoplasmic shuttling protein whose nuclear export is mediated by Xpo1 and Mex67 (1, 5). However, inhibition of transcription in *rpb1-1*^{ts} mutant cells (5) or incubation with thiolutin (Fig. 10B) does not result in nuclear accumulation of Pab1-GFP, suggesting that nuclear retention upon transcription inhibition is not a phenotype affecting all nucleocytoplasmic shuttling proteins or all mRNA binding proteins. Transcription inhibition also prevents GFP-Cth2 localization to P bodies in the *xrn1*Δ mutant strain (Fig. 10C). Interestingly, nuclear accumulation of GFP-Cth2 occurs in punctate structures in the mRNA export-deficient *mex67-5*^{ts} mutant strain at 37°C (Fig. 3B) and in wild-type cells treated with thiolutin (Fig. 10B). This localization likely corresponds to sites of retained polyadenylated mRNAs previously described (10, 25). Moreover, localization of Cth2 to these structures is independent of its ability to interact with mRNA since the non-mRNA-binding mutant protein GFP-Cth2-C190,213A accumulates in similar structures upon exposure to thiolutin (Fig. 10D). Together, these data are consistent with nucleocytoplasmic shuttling of Cth2 being important for the nuclear recruitment of target mRNAs for subsequent escort to the cytosol for degradation.

Nuclear recruitment of ARE-containing mRNAs targeted for degradation during Fe deficiency. Although several steps in the mechanisms of AMD have been characterized in mammals and in yeast, the site at which Cth2, TTP, and other related proteins encounter their cognate mRNAs for subsequent cytosolic degradation remains an unresolved question (4, 12, 13, 15). Similarly, little is known about the role of TTP and related proteins inside the nucleus. Recent studies identified Cth2 as a factor that regulates 3′-end processing by interfering with normal poly(A) site selection leading to the formation of extended mRNAs that are highly unstable (22). Cells expressing an allele of Cth2 in which the first 86 amino acids have been deleted accumulate extended *SDH4* transcripts. This observation suggests that the amino-terminally truncated form of Cth2 can bind and promote the formation of the extended mRNA but fails

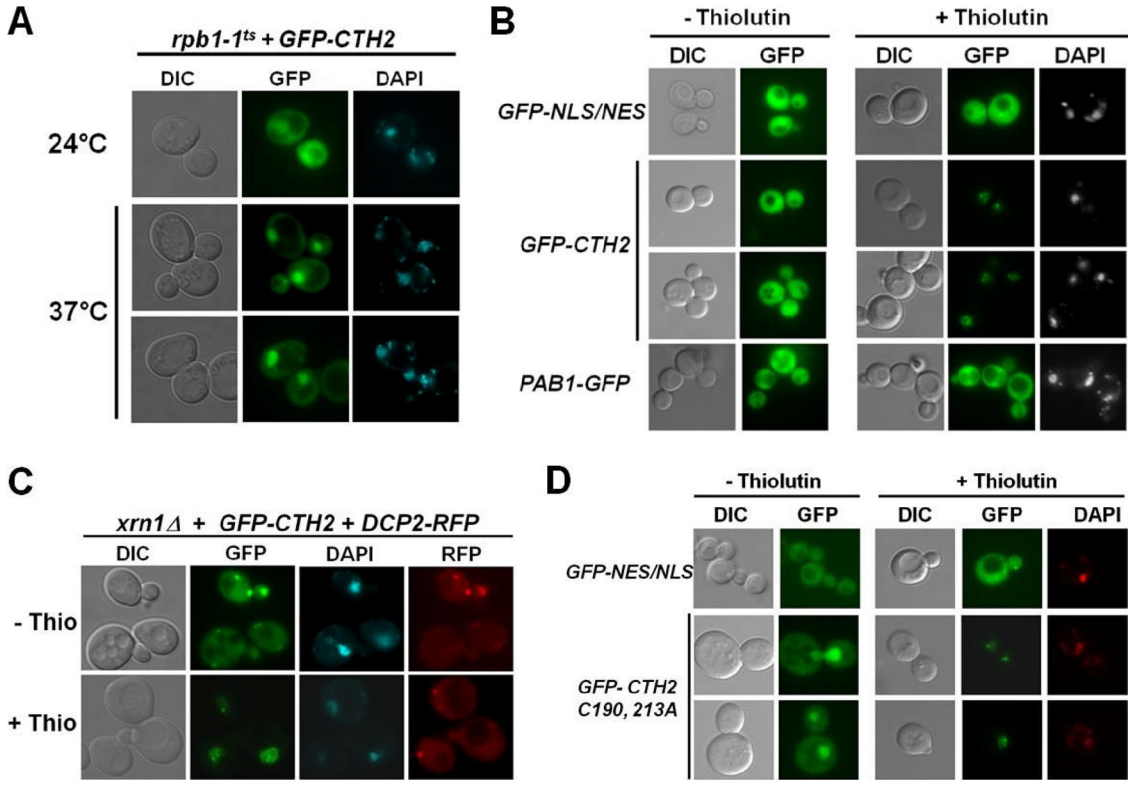

FIG. 10. Transcription-dependent shuttling of Cth2. (A) GFP-Cth2 is retained in the nuclei of cells defective in transcription. *rbp1-1*^{ts} cells transformed with pRS416-*GFP-CTH2* were visualized at 24°C and after a 1 h shift to 37°C to disrupt the activity of the thermosensitive allele of the largest subunit of RNA polymerase II, Rpb1-1. (B) *cth1*Δ *cth2*Δ mutant cells transformed with plasmid *GFP-NLS/NES*, pRS416-*GFP-CTH2* or *PAB1-GFP* were visualized before and after treatment with 5 μl/ml thiolutin for 30 min. (C) Transcription inhibition disrupts Cth2 localization to P bodies. *xrn1*Δ mutant cells coexpressing pRS416-*DCP2-RFP* and pRS416-*GFP-CTH2* were observed in the presence or absence of thiolutin treatment. (D) Nuclear accumulation of Cth2 to punctate structures is independent of mRNA-binding activity. *cth1*Δ *cth2*Δ mutant cells transformed with plasmid pRS416-*GFP-CTH2* or non-mRNA-binding plasmid pRS416-*GFP-CTH2-C190,213A* were visualized before and after treatment with thiolutin as in C.

to induce its rapid turnover (22). We deleted the amino-terminal 89 amino acids to generate the GFP-Δ89Cth2 mutant protein and established its subcellular localization by live fluorescence microscopy. Figure 11A demonstrates that our GFP-Δ89Cth2 fusion promotes the accumulation of extended *SDH4* transcripts, as described by Prouteau et al. (22). As shown in Fig. 11B, GFP-Δ89-Cth2 localized throughout cells and treatment with thiolutin induced its nuclear retention in a manner comparable to that of full-length GFP-Cth2 (Fig. 10B). To ascertain if truncation of the amino terminus of Cth2 affects its ability to accumulate in P bodies, we visualized the GFP-Δ89Cth2 protein in *xrn1*Δ mutant cells. As shown in Fig. 11C, the GFP-Δ89Cth2 protein colocalized with the P-body component protein Dcp2-RFP. Moreover, treatment with thiolutin led to its nuclear retention and loss of P-body localization, suggesting that failure of the Δ89Cth2 truncation to promote the rapid turnover of the extended transcripts is likely not a consequence of defects in shuttling or in localization to P bodies.

DISCUSSION

While members of the TTP family of proteins promote the accelerated degradation of their target mRNAs in the cytosol, localization studies revealed that TTP and family members are nucleocytoplasmic shuttling proteins. However, neither the function of nuclear TTP nor a role for TTP shuttling in AMD has been uncovered. Experimental results presented in this report indicate that nucleocytoplasmic shuttling of the TTP-homologous protein Cth2 is important for the nuclear recruitment of target mRNAs, perhaps cotranscriptionally, for escort to the cytosol for degradation under conditions of Fe starvation.

Our data indicate that Cth2, like its mammalian counterparts, is a nucleocytoplasmic shuttling protein. While the motif discovery algorithm PSORTII predicts the presence of an NLS sequence at the amino terminus of Cth2 (data not shown), the data presented in Fig. 5 demonstrate that the minimal region containing the nuclear import information of Cth2 is the mRNA-binding domain, as in TTP and related proteins. Thus, it is possible that the predicted NLS sequence at the amino terminus, if a bona fide localization sequence, plays only a minor role in the nuclear import of Cth2 or functions under a distinct set of conditions. TTP and related proteins are known to be exported from the nucleus via the NES-dependent pathway mediated by the nuclear export receptor Crm1/Xpo1 (21). Conversely, our results indicate that Cth2 export from the nucleus from *S. cerevisiae* is not under the direct regulation of this pathway. First, our efforts to identify an NES within Cth2

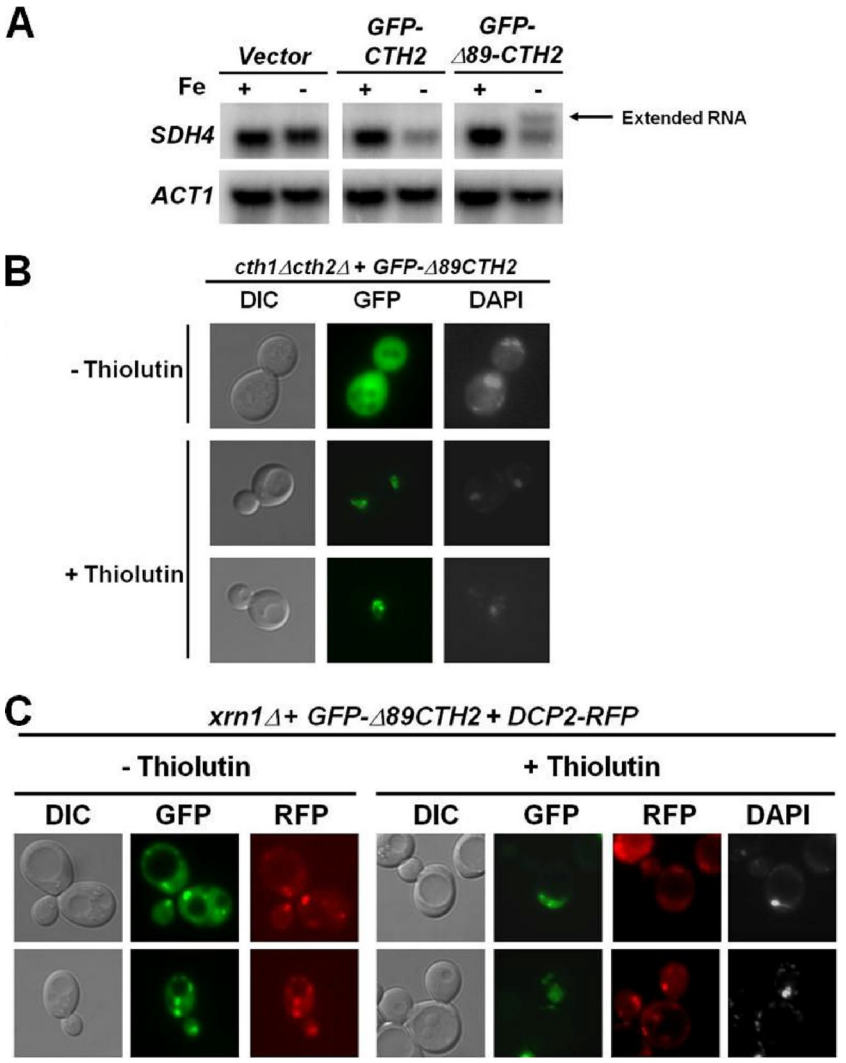

FIG. 11. Truncation of the amino terminus of Cth2 does not affect subcellular localization. (A) *cth1*Δ *cth2*Δ mutant cells transformed with vector alone, *GFP-CTH2* or *GFP-*Δ*89-CTH2* were grown under +Fe and −Fe conditions and total RNA was analyzed by RNA blotting. (B) *cth1*Δ *cth2*Δ and (C) *xrn1*Δ mutant cells transformed with *GFP-*Δ*89CTH2* were grown under −Fe conditions and visualized before or after treatment with 5 μl/ml thiolutin for 30 min.

by deletion mapping and site-directed mutagenesis of a putative sequence predicted by the NES discovery algorithm NES Finder were unsuccessful (data not shown). Second, localization experiments with strains defective in NES-dependent transport but proficient in mRNA export did not show any defects in the localization of GFP-Cth2. Moreover, localization of GFP-Cth2 in a yeast strain sensitive to disruption of Crm1/Xpo1 function by treatment with leptomycin B (T539C mutant) (18) also did not show altered localization of the fusion protein (data not shown). However, nuclear export of GFP-Cth2 is impaired in strains defective in mRNA export such the *xpo1-1*^{ts} and the *mex67-5*^{ts} mutant strains, and a mutant allele of Cth2 that fails to interact with mRNA also accumulates in the nuclei of wild-type cells. Taken together, our results demonstrate that Cth2 import into the nucleus is facilitated by its TZF domain and that nuclear export of Cth2 is dependent on nuclear mRNA export mechanisms and independent of the NES-mediated transport pathway.

Observations described here suggest that nucleocytoplasmic shuttling of Cth2 is important for the nuclear recruitment of target mRNAs for their efficient degradation in the cytosol. First, alterations of the steady-state localization of GFP-Cth2 causes defects in AMD and a growth deficiency under Fe starvation conditions. Second, a shift in the equilibrium of expression to either the nucleus or the cytosol prevents GFP-Cth2 from reaching P bodies in a *xrn1*Δ mutant strain. Interestingly, even the NES_2-GFP-Cth2 fusion shows impaired localization to P bodies, even though this fusion should have no defects in nuclear import. This observation likely reflects the inability of this protein to interact with mRNA as the appended NES_2 cassette drives the rapid export of the GFP-Cth2 fusion back out of the nucleus, thereby diminishing the opportunity for the fusion protein to interact with target transcripts (data not shown). Third, a non-mRNA-binding mutant allele of Cth2 cannot reach P bodies, even if its expression equilibrium is shifted to the cytosol by attachment of the NES_2 cas-

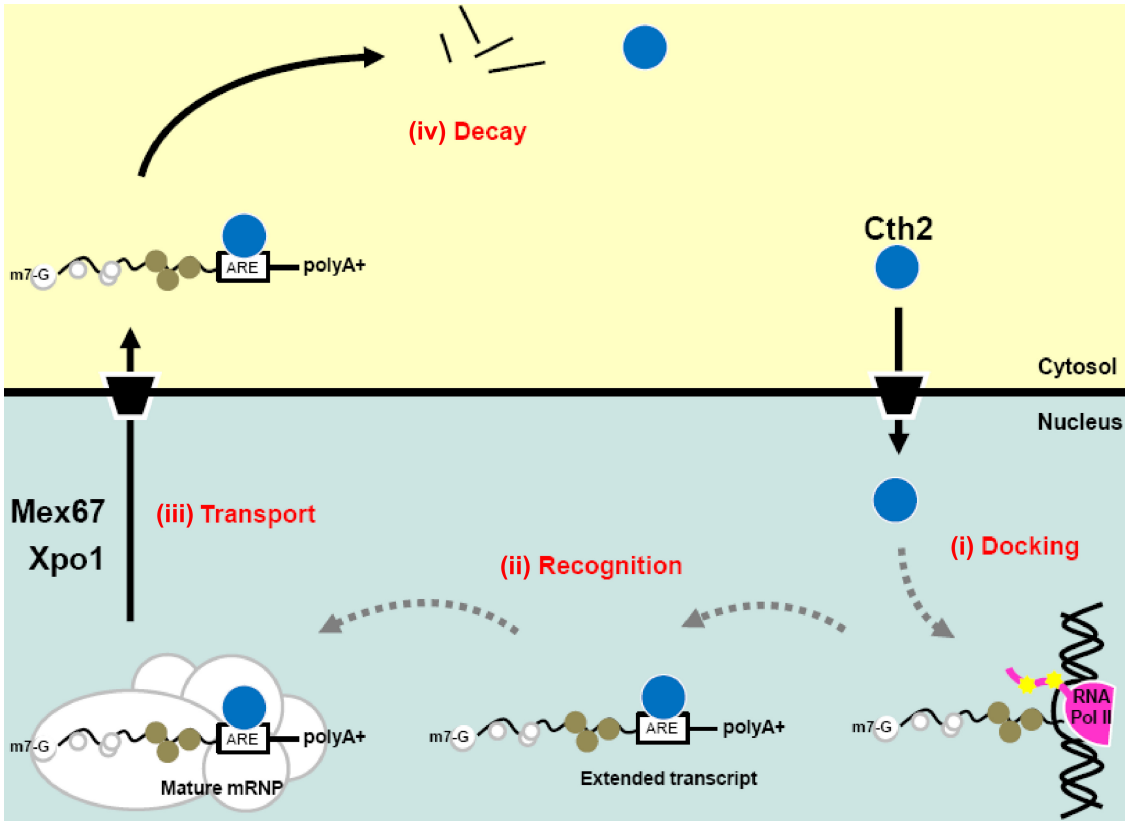

FIG. 12. Cth2 recruits target mRNAs in the nucleus for degradation in the cytosol during Fe deficiency. Steps in ARE mRNA recruitment: (i) docking: Cth2 (blue circle) is brought to target mRNAs by 3′-end processing factors; (ii) recognition: Cth2 binds AREs within target transcripts. Cth2 binding causes readthrough of normal polyadenylation site resulting in extended transcript formation (22); (iii) transport: mature mRNP containing extended target transcript bound by Cth2 is exported via mRNA export pathways; (iv) decay: Cth2 bound transcript is deadenylated and degraded in the cytosol. Factors involved in processing and cytosolic mRNA decay have been omitted for simplicity.

sette at its amino terminus. Fourth, disruption of transcription causes nuclear accumulation of GFP-Cth2 and prevents its localization to P bodies in the *xrn1*Δ mutant strain.

Deletion of the amino terminus of Cth2 eliminates its ability to degrade mRNA. We tested whether the inability of the GFP-Δ89Cth2 mutant to induce mRNA degradation was due to a defect in shuttling or a defect in P-body localization. However, our observations indicate that truncation of the amino terminus of Cth2 acts as a separation-of-function mutation that allows Cth2 to translocate into the nucleus, recognize and bind target transcripts, induce the formation of extended mRNA, and localize to P bodies but fails to promote degradation of the bound transcripts, perhaps due to its inability to recruit the deadenylase machinery. Nuclear magnetic resonance studies on the TZF domain of the TTP family member Tis11D, bound to the nonameric sequence 5′-$U_1U_2A_3U_4U_5U_6A_7U_8U_9$-3′, revealed that the second TZF interacts with the 5′-most $U_2A_3U_4U_5$ sequence, while the first TZF of the protein interacts with the 3′-most $U_6A_7U_8U_9$ region of the sequence (11). Therefore, the amino terminus of Tis11D would be oriented toward the poly(A) tail of the bound transcript. By analogy, this observation may suggest that the deadenylase is brought to the ARE-containing transcript through a direct or indirect interaction with the amino terminus of Cth2. In fact, work by Prouteau et al. (22) identified the region between amino acids 36 and 57 of Cth2 as essential in promoting the deadenylation of the *SDH4* mRNA. Interestingly, this 21-amino-acid region contains a predicted alpha helix which may act as a site for deadenylase recruitment.

Observations reported here and previous results prompt us to propose a working model for Cth2-mediated AMD in response to Fe deficiency in yeast that consists of the following four steps (Fig. 12). (i) In the docking step, Cth2 is recruited to the nascent mRNA before polyadenylation takes place. (ii) In the recognition step, the putative proximity of Cth2 to the 3′ end allows Cth2 to be deposited onto the nascent ARE sequence. (iii) In the transport step, target mRNA bound by Cth2 is packaged into a mature mRNP and exported to the cytosol via mRNA export pathways. (iv) In the decay step, Cth2 directs the bound transcript to the site of degradation in the cytosol. Evidence for a docking step comes from the observation that Cth2 affects poly(A) site selection (22), suggesting that Cth2 binds target ARE mRNAs at a step before polyadenylation. Factors involved in poly(A) tail regulation and mRNP export, such as Nab2 and Npl3, are cotranscriptionally recruited to the nascent mRNPs, and experiments have shown that inhibition of transcription disrupts their shuttling activity (8, 14). Since inhibition of transcription also disrupts Cth2 shuttling and causes the retention of Cth2 in nuclear foci independently of mRNA binding, this suggests a model

whereby Cth2 docks onto a site near the 3′ end prior to the synthesis of a nascent ARE sequence. Once the ARE sequence is transcribed, Cth2 could recognize and bind stably to the mRNA target, thereby preventing normal poly(A) site selection and inducing extended transcripts. mRNA surveillance mechanisms ensure that only properly processed mRNPs are exported to the cytoplasm. Our data suggest that while Cth2 promotes the formation of extended transcripts, these appear to be packaged into mature mRNPs and exported to the cytosol for degradation by components of the 5′→3′ decay machinery. Evidence for this comes from the observation that the separation-of-function mutant protein GFP-Δ89Cth2 is efficiently recruited to P bodies, though it fails to normally promote deadenylation and subsequent 5′→3′ degradation of the target mRNA. In addition, it is likely that degradation of at least a subgroup of Cth2 target mRNAs may involve the 3′→5′ decay pathway, although this remains to be fully investigated (our unpublished observations).

Our model raises the interesting possibility that the cytosolic fate of mRNAs encoding proteins involved in highly Fe-dependent processes is determined by Cth2 soon after transcription by promoting their selective delivery to the cytosol for degradation, ensuring a rapid response to Fe deficiency. Moreover, our data revealed differences in posttranslational modifications of nuclear versus cytosolic Cth2, which could be one of several regulatory mechanisms of the protein. Studies aimed at understanding the role of posttranslational modifications, such as phosphorylation, in Cth2 function and regulation are under way.

ACKNOWLEDGMENTS

We are grateful to Jack Keene and Roy Parker for helpful discussions and comments on the manuscript and to Sam Johnson and Yasheng Gao at the Duke Light Microscopy Facility for advice. We thank Roy Parker for providing the DCP2-RFP plasmid; Karsten Weis for providing the GFP-NES/NLS plasmid and the *mex67-5*^{ts}, *xpo1-1*^{ts}, *mex67-5*/*xpo1-1*, and *rbp1-1*^{ts} mutant strains; Anita Corbett for the *YAP1-GFP* plasmid and the *crm1-2* and *crm1-3* mutant strains; and Maurice Swanson for pPAB1-GFP.

S.V.V. is a trainee of the Duke University Program in Genetics and Genomics. This work was supported by NIH grant GM41840 to D.J.T., NIH predoctoral fellowship FDK081304A to S.V.V., and BIO2008-02835 to S.P.

REFERENCES

1. **Brune, C., S. E. Munchel, N. Fischer, A. V. Podtelejnikov, and K. Weis.** 2005. Yeast poly(A)-binding protein Pab1 shuttles between the nucleus and the cytoplasm and functions in mRNA export. RNA **11:**517–531.
2. **Carballo, E., W. S. Lai, and P. J. Blackshear.** 2000. Evidence that tristetraprolin is a physiological regulator of granulocyte-macrophage colony-stimulating factor messenger RNA deadenylation and stability. Blood **95:**1891–1899.
3. **Carballo, E., W. S. Lai, and P. J. Blackshear.** 1998. Feedback inhibition of macrophage tumor necrosis factor-alpha production by tristetraprolin. Science **281:**1001–1005.
4. **Chen, C. Y., et al.** 2001. AU binding proteins recruit the exosome to degrade ARE-containing mRNAs. Cell **107:**451–464.
5. **Dunn, E. F., C. M. Hammell, C. A. Hodge, and C. N. Cole.** 2005. Yeast poly(A)-binding protein, Pab1, and PAN, a poly(A) nuclease complex recruited by Pab1, connect mRNA biogenesis to export. Genes Dev. **19:**90–103.
6. **Edgington, N. P., and B. Futcher.** 2001. Relationship between the function and the location of G1 cyclins in S. cerevisiae. J. Cell Sci. **114:**4599–4611.
7. **Fenger-Grøn, M., C. Fillman, B. Norrild, and J. Lykke-Andersen.** 2005. Multiple processing body factors and the ARE binding protein TTP activate mRNA decapping. Mol. Cell **20:**905–915.
8. **Green, D. M., et al.** 2002. Nab2p is required for poly(A) RNA export in Saccharomyces cerevisiae and is regulated by arginine methylation via Hmt1p. J. Biol. Chem. **277:**7752–7760.
9. **Hentze, M. W., M. U. Muckenthaler, and N. C. Andrews.** 2004. Balancing acts: molecular control of mammalian iron metabolism. Cell **117:**285–297.
10. **Hilleren, P., and R. Parker.** 2001. Defects in the mRNA export factors Rat7p, Gle1p, Mex67p, and Rat8p cause hyperadenylation during 3′-end formation of nascent transcripts. RNA **7:**753–764.
11. **Hudson, B. P., M. A. Martinez-Yamout, H. J. Dyson, and P. E. Wright.** 2004. Recognition of the mRNA AU-rich element by the zinc finger domain of TIS11d. Nat. Struct. Mol. Biol. **11:**257–264.
12. **Lai, W. S., et al.** 1999. Evidence that tristetraprolin binds to AU-rich elements and promotes the deadenylation and destabilization of tumor necrosis factor alpha mRNA. Mol. Cell. Biol. **19:**4311–4323.
13. **Lai, W. S., E. A. Kennington, and P. J. Blackshear.** 2003. Tristetraprolin and its family members can promote the cell-free deadenylation of AU-rich element-containing mRNAs by poly(A) ribonuclease. Mol. Cell. Biol. **23:**3798–3812.
14. **Lee, M. S., M. Henry, and P. A. Silver.** 1996. A protein that shuttles between the nucleus and the cytoplasm is an important mediator of RNA export. Genes Dev. **10:**1233–1246.
15. **Lykke-Andersen, J., and E. Wagner.** 2005. Recruitment and activation of mRNA decay enzymes by two ARE-mediated decay activation domains in the proteins TTP and BRF-1. Genes Dev. **19:**351–361.
16. **Massé, E., and M. Arguin.** 2005. Ironing out the problem: new mechanisms of iron homeostasis. Trends Biochem. Sci. **30:**462–468.
17. **Murata, T., Y. Yoshino, N. Morita, and N. Kaneda.** 2002. Identification of nuclear import and export signals within the structure of the zinc finger protein TIS11. Biochem. Biophys. Res. Commun. **293:**1242–1247.
18. **Neville, M., and M. Rosbash.** 1999. The NES-Crm1p export pathway is not a major mRNA export route in Saccharomyces cerevisiae. EMBO J. **18:**3746–3756.
19. **Neville, M., F. Stutz, L. Lee, L. I. Davis, and M. Rosbash.** 1997. The importin-beta family member Crm1p bridges the interaction between Rev and the nuclear pore complex during nuclear export. Curr. Biol. **7:**767–775.
20. **Pedro-Segura, E., et al.** 2008. The Cth2 ARE-binding protein recruits the Dhh1 helicase to promote the decay of succinate dehydrogenase SDH4 mRNA in response to iron deficiency. J. Biol. Chem. **283:**28527–28535.
21. **Phillips, R. S., S. B. Ramos, and P. J. Blackshear.** 2002. Members of the tristetraprolin family of tandem CCCH zinc finger proteins exhibit CRM1-dependent nucleocytoplasmic shuttling. J. Biol. Chem. **277:**11606–11613.
22. **Prouteau, M., M. C. Daugeron, and B. Seraphin.** 2008. Regulation of ARE transcript 3′ end processing by the yeast Cth2 mRNA decay factor. EMBO J. **27:**2966–2976.
23. **Puig, S., E. Askeland, and D. J. Thiele.** 2005. Coordinated remodeling of cellular metabolism during iron deficiency through targeted mRNA degradation. Cell **120:**99–110.
24. **Puig, S., S. V. Vergara, and D. J. Thiele.** 2008. Cooperation of two mRNA-binding proteins drives metabolic adaptation to iron deficiency. Cell Metab. **7:**555–564.
25. **Segref, A., et al.** 1997. Mex67p, a novel factor for nuclear mRNA export, binds to both poly(A)+ RNA and nuclear pores. EMBO J. **16:**3256–3271.
26. **Shakoury-Elizeh, M., et al.** 2004. Transcriptional remodeling in response to iron deprivation in Saccharomyces cerevisiae. Mol. Biol. Cell **15:**1233–1243.
27. **Stade, K., C. S. Ford, C. Guthrie, and K. Weis.** 1997. Exportin 1 (Crm1p) is an essential nuclear export factor. Cell **90:**1041–1050.
28. **Stoecklin, G., et al.** 2002. Functional cloning of BRF1, a regulator of ARE-dependent mRNA turnover. EMBO J. **21:**4709–4718.
29. **Stoecklin, G., P. Stoeckle, M. Lu, O. Muehlemann, and C. Moroni.** 2001. Cellular mutants define a common mRNA degradation pathway targeting cytokine AU-rich elements. RNA **7:**1578–1588.
30. **Taylor, G. A., M. J. Thompson, W. S. Lai, and P. J. Blackshear.** 1996. Mitogens stimulate the rapid nuclear to cytosolic translocation of tristetraprolin, a potential zinc-finger transcription factor. Mol. Endocrinol. **10:**140–146.
31. **Vasudevan, S., and S. W. Peltz.** 2001. Regulated ARE-mediated mRNA decay in Saccharomyces cerevisiae. Mol. Cell **7:**1191–1200.
32. **Vergara, S. V., and D. J. Thiele.** 2008. Post-transcriptional regulation of gene expression in response to iron deficiency: coordinated metabolic reprogramming by yeast mRNA-binding proteins. Biochem. Soc. Trans. **36:**1088–1090.